PHYSICAL REVIEW B VOLUME 11, NUMBER 12 15 JUNE 1975

Generalized-Wannier-function solutions to model surface potentials

J. G. Gay and J. R. Smith
Research Laboratories, General Motors Corporation, Warren, Michigan 48090
(Received 23 December 1974)

The generalized-Wannier-function (GWF) formalism is used to calculate the electronic structure associated with the lowest bands of several one-dimensional model surfaces. The results are compared with exact solutions obtained independently. The GWF calculations, which are variational in nature, are found to give very satisfactory accuracy with simple trial functions which employ, at most, four variational parameters. The GWF's damp very rapidly to the bulk Wannier function. Only those in the two lattice sites closest to the surface are significantly different. This implies, for filled bands, a similar rapid damping of the charge density. These facts, which might be anticipated for tightly bound electrons, hold even in the case of weak pontentials in which the electrons are nearly free.

I. INTRODUCTION

The usual way to develop a theoretical description of a system of electrons is to calculate eigenfunctions of the Schrödinger equation. This has proven satisfactory for small systems (atoms and molecules) and for infinite systems which are periodic (bulk solids). However, when the translational symmetry of a solid is interrupted by a surface the resulting system is neither small nor fully periodic, and methods which depend on either of these aspects are not suitable for calculating the eigenfunctions. The eigenfunctions as well as the methods used to calculate them become intrinsically more complicated. In addition to the possibility of surface states localized in the surface region, the bulk states are everywhere changed in order to satisfy the boundary conditions imposed by the surface. Thus, from the point of view of the eigenfunctions, the effects of the surface persist indefinitely into the crystal bulk.

On the other hand, there is ample experimental evidence that the effects of a surface on such observables as charge densities and local densities of states, while locally strong, are rapidly damped so that they quickly revert to their bulk values. The evidence is especially apparent in recent experiments on the elemental semiconductors. Ion-neutralization spectroscopy, which probes essentially only the surface layer of atoms, can give electron energy distributions which are qualitatively different from the bulk density of states,[1] whereas in ultraviolet photoemission spectroscopy, the electron energy distributions are dominated by the bulk density of states even under conditions in which the experiment probes only about four atom layers.[2]

This suggests that there may be an inherent advantage to a description of the electronic structure in terms of local functions which share with the observables a rapid return to bulk behavior. With such a description a surface calculation would involve only the determination of those functions in the immediate vicinity of the surface which differ from the local functions of the bulk.

The generalized-Wannier-function concept, recently introduced by Kohn and Onffroy,[3] describes the electronic structure exactly in terms of local functions *which may be calculated directly without first calculating wave functions*. Generalized Wannier functions (GWF's) are the counterparts for crystals with defects of the familiar Wannier functions of perfect crystals. They are atomiclike functions localized about the lattice sites of the system and represent an alternative basis for the description of the electronic structure of the defect problem. A single set of GWF's is sufficient to describe an entire perturbed band. Only those GWF's near the defect need be different from the Wannier functions of the perfect crystal, and they may be calculated by a variational procedure which minimizes the total energy of the perturbed band.

This paper describes calculations on one-dimensional model surfaces designed to test the GWF formalism as a practical tool for the calculation of surface electronic structure. We wish to answer such questions as how many GWF's in the surface region must differ from the bulk Wannier function, and how accurate are the calculations when simple trial functions are used in the variational calculation. This is necessary information for the practitioner which is needed in addition to the theorems on asymptotic localization, and asymptotic decay to the bulk Wannier functions proved for GWF's of one-dimensional systems.[3-5] Some of the material presented here has been reported previously.[6] General properties

for three-dimensional systems have been considered in a separate publication.[7]

There are several reasons for doing these first GWF calculations on simple one-dimensional systems. The calculations are relatively easy to do, and the results are easily interpreted and displayed. However, the principal advantage is that the GWF calculations can be tested absolutely for accuracy by comparing them with the exact solutions. The latter can be always found for one-dimensional systems by numerical integration or otherwise.

The GWF formalism is briefly set forth in Sec. II. The test calculations are presented in Sec. III along with the evaluation of their accuracy. The results are summarized and discussed in Sec. IV.

II. GENERALIZED WANNIER FUNCTIONS

We outline the GWF formalism in the context of the one-dimensional-model-surface problem with emphasis on calculational aspects. The formalism proceeds on the assumption, customarily employed in the band theory of solids, that electrons are adequately described by an effective, local, one-electron potential. We deal therefore with a one-electron problem,

$$H\phi_q(x) = E_q\phi_q(x), \tag{2.1}$$

where (in the text rydberg units are used for the energy and atomic units for length)

$$H = -\frac{d^2}{dx^2} + V(x), \tag{2.2}$$

and where $V(x)$ is a model surface potential. Examples of $V(x)$ are shown in Fig. 1. The $\phi_q(x)$ are the wave functions of a single perturbed band and q is an intraband quantum number. Note that this perturbed band may contain surface states localized near the surface as well as unlocalized band states.

The GWF theory asserts that there is a set of orthonormal generalized Wannier functions, $a_n(x)$, localized about the lattice sites of the system (the potential minima of Fig. 1) such that for all $\phi_q(x)$,

$$\phi_q(x) = \sum_n C_{q,n}a_n(x). \tag{2.3}$$

The index n may normally be regarded as a lattice vector measured from the surface site, but if, e.g., the potential well nearest the surface is very shallow or very deep there may be no GWF's or more than one GWF associated with that site.

The $a_n(x)$ of the one-dimensional-surface problem have been analyzed by Rehr and Kohn[5] who show that, asymptotically, the $a_n(x)$ can be exponentially localized. Further, for lattice sites n asymptotically far from the surface, the $a_n(x)$ approach the $a_n^0(x)$ exponentially in n, where the $a_n^0(x)$ are the Wannier functions of the periodic system with potential $V^0(x)$.

From a practical standpoint, an important feature of the GWF's is that they may be calculated directly by a variational procedure.[3,7] The procedure hinges on the unitary relation (2.3). Because of this the total band energy (we assume a filled band)

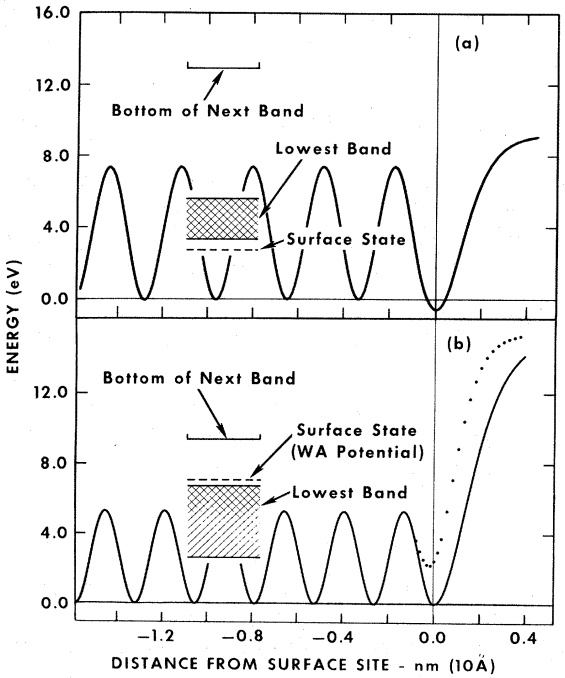

FIG. 1. Illustration of the three potentials used in the calculations. (a) Shows the SB potential. The strength parameter of the Mathieu potential is $l = 2^{1/4}$. To achieve realistic lattice constants and energies, a value of 5 was used for the scaling parameter t. The Mathieu lattice constant is then $d = 0.3146$ nm (5.946 a.u.). The well parameters are $\lambda = 2.527\times10^5$ eV nm^{-2}, $b = 0.1573$ nm, $\mu = 0$, and $U_0 = -0.5718$ eV. The potentials are matched at $x_0 = -0.05292$ nm. The relevant part of the energy spectrum is shown in the inset. The surface state split off from the bottom of the first band is a consequence of the deep surface well. (b) Shows the WN potential (solid curve), and the WA potential (dotted curve). Both potentials employ a Mathieu potential with $l = 1$. Again, $t = 5$ so that $d = 0.2646$ nm (5 a.u.). For the WN potential this Mathieu potential is matched, at $x_0 = 0$, to a well potential with parameters $\lambda = 2.429\times10^5$ eV nm^{-2}, $b = 0.01984$ nm, $\mu = 0$, and $U_0 = 0$. For the WA potential, $x_0 = 0.07938$ nm, $\lambda = 3.498\times10^5$ eV nm^{-2}, $b = 0.1323$ nm, $\mu = 0.15$, and $U_0 = 2.264$ eV. The energy spectra are shown in the inset. The shallow surface well of the WA potential causes a surface state to split off from the top of the lowest band as indicated.

$$\Omega = \sum_q E_q \tag{2.4}$$

may be written

$$\Omega = \sum_n \langle a_n(x)|H|a_n(x)\rangle \ . \tag{2.5}$$

It is this quantity in the form (2.5) which is minimized variationally to determine the $a_n(x)$. In practice, one does not have to deal with the infinite sum (2.5) but with a truncated sum of m terms,

$$\Omega_m = \sum_{n=1}^{m} \langle a_n(x)|H|a_n(x)\rangle \ , \tag{2.6}$$

where m is a site which is in the bulk, i.e., is such that all terms deleted from (2.5) are equal to $\langle a_m(x)|H|a_m(x)\rangle$ to sufficient accuracy. This is so because

$$a_n(x) \cong a_n^0(x), \quad n \geq m \ . \tag{2.7}$$

Thus the number of distinct GWF's to be determined is finite.

The minimization of (2.6) must be done subject to the constraint that the GWF's be orthonormal,

$$\langle a_n(x)|a_{n'}(x)\rangle = \delta_{nn'} \ . \tag{2.8}$$

These constraints[8] can be imposed in the following way.[9,3] One makes up the trial $a_n(x)$ from a set of functions $g_n(x)$ generally more localized than the $a_n(x)$ and not orthonormal,[10]

$$\langle g_n(x)|g_{n'}(x)\rangle = G_{nn'} \ . \tag{2.9}$$

The trial $a_n(x)$ are then constructed by the symmetric orthogonalization procedure,[11]

$$a_n(x) = \sum_{n'} G_{n,n'}^{-1/2} g_{n'}(x), \tag{2.10}$$

so that Ω_m may be written

$$\Omega_m = \sum_{n=1}^{m} \sum_{l,l'} G_{n,l}^{-1/2} G_{n,l'}^{-1/2} \langle g_l(x)|H|g_{l'}(x)\rangle \ . \tag{2.11}$$

The procedure described above implies that the variational calculation is done by increasing the value of m in (2.6) until $a_m(x)$ stabilizes to the bulk Wannier function $a_m^0(x)$. This is essentially what we do but we find it is helpful and perhaps more efficient to calculate the bulk Wannier function first and use it as a reference in calculating the GWF's which are perturbed by the surface. This is the approach taken in Sec. III. The bulk calculation is relatively simple. Because all lattice sites are equivalent, there is only one $a_n^0(x)$ (that is, $a_{n'}^0$ differs from a_n^0 only by being displaced from n to n') and only one $g_n^0(x)$. The energy to be minimized reduces to a single matrix element,[9]

$$\Omega^0 = \langle a_n^0(x)|H^0|a_n^0(x)\rangle = \sum_{ll'} (G_{nl}^0)^{-1/2}(G_{nl'}^0)^{-1/2}\langle g_l^0(x)|H^0|g_{l'}^0(x)\rangle \ . \tag{2.12}$$

In (2.12) H^0 is the bulk Hamiltonian containing the periodic V^0, and n is an arbitrary lattice point.

There are several practical advantages to this method of handling the constraints. The g's are not required to be orthogonal and, in contrast to the a's, oscillations on neighboring sites are not introduced by an orthogonality requirement. The g's are thus simpler functions than the a's and may be described with fewer parameters. Further, these parameters may be varied independently in minimizing Ω_m. Finally the sharper localization of the g's means that they revert to bulk behavior even more rapidly than the a's. There is a disadvantage, however, in that the parameters which define the g's appear nonlinearly in (2.11) and Ω_m must be minimized by a direct-search process.[9]

After calculating GWF's for the model surfaces by the procedure just described we will test the accuracy of the variational calculations by comparing wave functions to exact solutions obtained independently as described in Sec. III. To make this comparison it is necessary to calculate approximate wave functions from the GWF's. The rather extensive discussion involving wave functions may leave the impression that one must calculate wave functions in order to extract physical observables from the GWF's. We wish to emphasize that this is *not* the case. One may calculate certain observables directly from the GWF's, notably the charge density and the local density of states, without calculating wave functions.[3,7,12] This holds true even for metals with unfilled bands.[13] Thus the GWF formalism appears to offer advantages in the self-consistency problem.

III. TEST CALCULATIONS

A. Model surface potentials

In Sec. III A we discuss the actual potentials used in the test calculations: how they are constructed, the methods of calculating the exact solutions, and how to characterize the potentials as to whether electrons are strongly or weakly attracted to the individual lattice sites.

The three potentials which we consider are shown in Fig. 1. Each of these is made up of two parts joined at a boundary point x_0 located near the surface-well minimum. To the left of x_0 the potential is a Mathieu potential of the form

$$V^0(x) = \sigma^2 d^2\{1 - \cos[2\pi(x - x')/d]\}, \tag{3.1}$$

while to the right it is a potential well of the form[14]

$$U(x) = \lambda b^2 \cosh^2\mu\{\tanh[(x-x'')/b - \mu] + \tanh\mu\}^2 + U_0. \tag{3.2}$$

The constants x', x'', and U_0 in Eqs. (3.1) and (3.2) are determined so that the potential is continuous with continuous derivative.

The solutions to the Mathieu equation

$$\left(-\frac{d^2}{dx^2} + V^0(x)\right)\phi^0(x) = E\phi^0(x) \tag{3.3}$$

are well known and their implications with regard to the band structure of solids has been exhaustively discussed by Slater.[15,16] The parameterization employed in (3.1) follows Halpern.[17] The parameter d is the lattice constant.

The potential $V^0(x)$ is so constructed that its curvature at a minimum is independent of d. Because of this it may be shown[16] that the wave functions $\phi^0(x)$ become independent of d, for large d. In this extreme tight-binding limit, the $\phi^0(x)$ become harmonic-oscillator wave functions which are the analogs of atomic wave functions for the Mathieu potential.

The potential well $U(x)$ in (3.2) behaves as follows. It has a minimum of U_0 at $x = x''$, rises asymptotically to $\lambda b^2 e^{2\mu} + U_0$ for positive x and to $\lambda b^2 e^{-2\mu} + U_0$ for negative x. λ directly controls the well depth, b its width, and μ how much it is skewed.[14] The well is symmetric for $\mu = 0$. There are solutions to the Schrödinger equation with this well potential which decay exponentially as $x \to +\infty$ for all energies in the range $U_0 \leq E < \lambda b^2 e^{2\mu} + U_0$. They may be expressed as combinations of exponentials and the hypergeometric function.[14] The range $U_0 \leq E < \lambda b^2 e^{-2\mu} + U_0$ spans all energies considered for the surface problems. For energies in one of its bands, the solutions of the Mathieu equation are Bloch waves of plus and minus k. Thus for any energy in a band, the logarithmic derivative of the well solution at x_0 can be matched by an appropriate linear combination of the Bloch waves to form a single currentless scattering state of the surface problem. Note that these band states may be indexed by the magnitude of k. In addition to the band states there may be special energies in the forbidden gaps of the Mathieu equation where the logarithmic derivative of the well solution is exactly equal, at x_0, to that of the solution to the Mathieu equation which decays to zero at $-\infty$. The solutions in the two regions can then be joined to form a solution localized in the surface region. These are the surface states of the model potential.

While the exact band states were obtained by matching known solutions as just described, as a matter of expedience, surface states were obtained by numerically integrating the well solution into the Mathieu region. The surface-state energies were determined by the requirement that the numerical solutions have the known form of the solution to the Mathieu equation which vanishes as $x \to -\infty$.

These one-dimensional potentials can be changed in two entirely different ways. Their strength may be increased or decreased, or they may be scaled. The strength of a potential involves the degree to which an electron in a given well is isolated from electrons in adjacent wells. This is a function of the depths of the wells relative to their separation and is measured, e.g., by the ratio of the first band gap to the width of the first band. Scaling, on the other hand, merely alters characteristic lengths and energies associated with a potential of a given strength. To illustrate these points we introduce the alternative parameterization of the Mathieu Hamiltonian (similar considerations apply to the full surface Hamiltonians),

$$H^0(t, l) = \frac{d^2}{dx^2} + \frac{\pi^2}{2}\frac{l^2}{t^2}\left(1 - \cos\frac{2\pi x}{lt}\right). \tag{3.4}$$

In (3.4), l is the strength parameter and t the scaling parameter. The relationships to the original parameters are

$$d = lt,$$
$$\sigma^2 = t^{-4}\pi^2/2. \tag{3.5}$$

l is related to Slater's[15,16] parameter s: $l = s^{1/4}$.

To illustrate that t scales the Hamiltonian (3.4) we make the change of variable $y = x/t$. Then,

$$H^0(l, t) = \frac{1}{t^2}\left[\frac{-d^2}{dy^2} + \frac{\pi^2 l^2}{2}\left(1 - \cos\frac{2\pi y}{l}\right)\right]$$
$$= \frac{1}{t^2}H^0(l, 1). \tag{3.6}$$

Thus the eigenvalues of $H^0(l, t)$ are t^{-2} times those of $H^0(l, 1)$. Ratios of eigenvalues and the strength of the potential are unaffected. As we will see, appropriate values for the strength parameter are of the order of unity, so that $t \sim 5$ produces realistic values: lattice constants $d \sim 5$ a.u. and characteristic energies ~ 0.5 Ry.

Let us now characterize the three specific potentials of Fig. 1. The test calculations involve the lowest perturbed bands of these potentials (shown in the insets of the figure) and the characterization therefore is based on the properties of these bands.

The potential of Fig. 1(a) has a relatively strong Mathieu potential ($l = 2^{1/4}$) and a surface state below the first Mathieu band. We term this potential the SB potential: S for "strong" and B for "below."

A rationale for gauging the strength of Mathieu potentials is discussed below. The two other potentials are displayed in Fig. 1(b). Both have the same Mathieu potential with $l = 1$. This Mathieu potential is relatively weak. These two potentials differ in their surface-well characteristics. The solid curve has a surface well of the same depth as the Mathieu wells and has no surface state. We term this the WN potential. The dotted curve shows the WA potential which has a shallow-surface well and a surface state above the first Mathieu band.

We now turn to the question of how to gauge the strength of the surface potentials. This is important because the test calculations will have little significance if the potentials are unrealistically strong. This is because electrons in adjacent potential wells become increasingly isolated from one another with increasing strength. The GWF calculation for the first band then approaches a limit in which it is simply a variational calculation of the lowest bound state of each of the isolated wells, a patently practical calculation.

Reference to Fig. 1 shows that the first band of even the SB potential has substantial width indicating appreciable interaction between wells. In Slater's analysis[15,16] of the $l = 1$ (his $s = 1$) Mathieu potential, he shows that the electrons of the first band are nearly free in the classic sense, that the wave functions are predominantly single plane waves except near the Brillouin-zone edges at $k = \pm \pi/d$. The transition from tight-binding to nearly-free behavior in the first band occurs in the range $1 \leq l \leq 1.5$ ($1 \leq s \leq 5$). This is apparent from Slater's plot (Fig. 6.3 of Ref. 15, or Fig. 2 of Ref. 16) of the Mathieu energy bands versus lattice constant. Thus our potentials, with $l = 2^{1/4} \approx 1.2$ and $l = 1$, are both more nearly-free-electron-like than tight binding.

One may make a connection with three-dimensional systems by constructing a three-dimensional separable Mathieu potential from V^0:

$$\mathcal{V}^0(x, y, z) = V^0(x) + V^0(y) + V^0(z) . \tag{3.7}$$

Such multidimensional Mathieu potentials have been discussed by Slater.[15,16] The Brillouin zone is simple cubic and the band structure of $\mathcal{V}^0$ is related to that of V^0 by

$$\epsilon^0_{\alpha\beta\gamma}(k_x, k_y, k_z) = E^0_\alpha(k_x) + E^0_\beta(k_y) + E^0_\gamma(k_z), \tag{3.8}$$

where α, β, and γ are one-dimensional band indices. The first band of $\mathcal{V}^0$ is ϵ_{111}, made up of the first bands of the three constituent potentials. The next band is threefold degenerate, consisting of ϵ_{211}, ϵ_{121}, and ϵ_{112}, and so on. For the three-dimensional S potential the ratio of first band gap to first bandwidth is 0.4. For reference, the ratio for diamond in 0.2.[18] The three-dimensional W potential has no band gap and, in fact, the s-type lowest band is substantially overlapped by the three degenerate p-type bands. The ratio of overlap to s bandwidth is 0.4, very nearly the same as the ratio for sodium (Ref. 15, p. 210).

This discussion of three-dimensional potentials is brought up to demonstrate that the two Mathieu potentials used in the surface potentials are on either side of the meaningful range of potential strengths. This is the justification for the characterization "strong" for the S potential and "weak" for the W potentials. There is of course no detailed resemblance to real three-dimensional potentials.

B. GWF calculations

In this part we employ the variational procedure described in Sec. II to calculate GWF's for the three model surface problems.

The aim of the test calculations is to determine if the GWF approach has potential as a practical tool for surface calculations. This will only be the case if it is possible to obtain satisfactory results with simple local functions whose form can be inferred from the wave functions of the constituent atoms. Otherwise the variational calculation will likely prove prohibitively difficult. The analog in the test calculations is that satisfactory accuracy be obtained with ground-state harmonic-oscillator wave functions (simple Gaussians) as the local functions.

Consequently we have carried out calculations on the model potentials using as local functions,

$$g_n(x) = (\alpha_n/\pi^{1/2})^{1/2} e^{-\alpha_n^2 (x-n)^2/2} , \tag{3.9}$$

where the α_n are the variational parameters. For the calculation of the bulk Wannier function a single function $g^0_n(x)$ is required. This single-parameter bulk calculation represents a small part of the entire GWF calculation, and is a repetition of the calculation of Halpern.[17] Most of the Hamiltonian and overlap matrix elements involved in the energy expressions (2.11) and (2.12) were done in closed form, and the entire calculation is a relatively simple affair. The results of these calculations are presented in Figs. 2 and 3 as plots of the GWF's in the surface region of the three potentials.

The very rapid damping of the GWF's to the bulk Wannier function which is apparent in Figs. 2 and 3 has very favorable implications for the GWF approach. The GWF's at the surface sites have smoothly decaying tails on their right or vacuum side but the characteristic Wannier-function oscillations on their left or crystal side. On

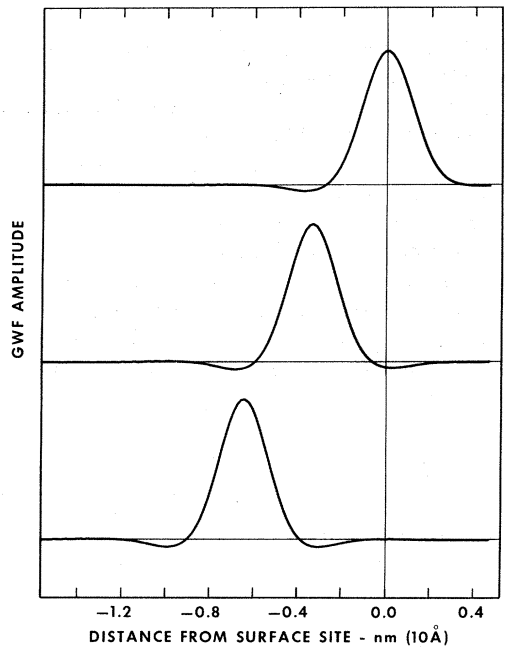

FIG. 2. GWF's computed with Gaussians for the first three lattice sites of the SB potential. The maxima of the GWF's lie very close to the minima of the successive potential wells of Fig. 1(a). By the third site the GWF has essentially stabilized to the bulk Wannier function.

moving into the crystal this asymmetry very rapidly disappears so that by the third site the GWF's are essentially equal to the bulk Wannier function. This is despite the fact that the surface is a massive perturbation of the bulk, and is true even for the W potentials which are nearly-free-electron-like in the sense discussed earlier. For filled bands, the electron charge density is given as the sum of the squares of the amplitudes of the GWF's.[3,7] Thus the charge density also damps very rapidly to the bulk charge density.[6]

The utility of the rapid damping shows up in the parameters α_n of the $g_n(x)$ plotted in Fig. 4. In principle these will differ from the bulk α for any finite n. However, for the W potentials, it was found sufficient to vary only the three α's closest to the surface from the bulk value. For the stronger SB potential only two α's needed to be different from the bulk value. For example, tests with the WA potential showed that when α_4 was allowed to vary it changed only slightly (from $0.690\pi/d$ to $0.6925\pi/d$), and introduced negligible changes in the GWF's. Notw that the damping of the α's is not necessarily exponential in n for any of the potentials and is not even monotonic for the WN potential. This is not in disagreement with the results of Ref. 5, which apply to asymptotic behavior ($n\to\infty$). We regard this demonstration of very rapid damping of the GWF's as one of the two principal consequences of these test calculations. The other is that quite satisfactory accuracy is obtained with simple atomlike functions for the $g_n(x)$, which we will demonstrate in Sec. III C.

Observe that, while the WN and WA potentials are locally quite different, their GWF's are notably similar. In fact, the main apparent difference is that the GWF for the surface site of the WA potential is displaced from the origin. This is because the surface well of this potential is displaced. Even though the GWF's of these potentials are very similar, there is a surface state for the WA potential but not for the WN potential as will be seen Sec. III C. This illustrates a point, which we believe will generally be true, that the GWF's will be less affected by a local perturbation than the wave functions.

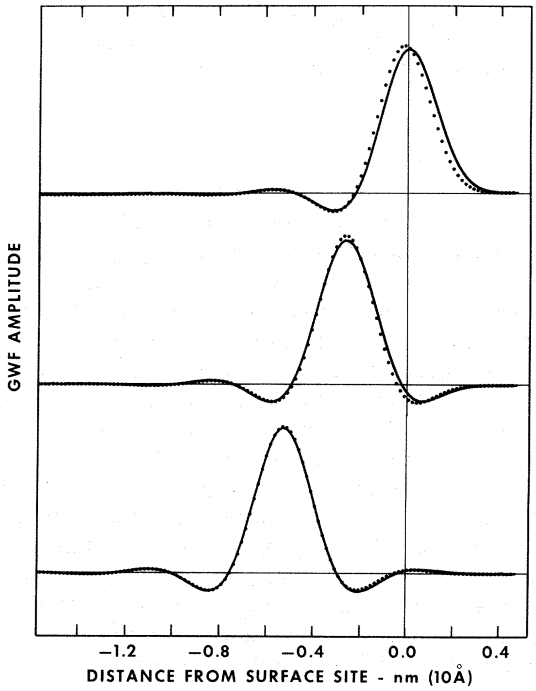

FIG. 3. GWF's computed with Gaussians for the first three lattice sites of the WN potential (solid curve) and WA potential (dotted curve). The decreased strength of these potentials relative to the SB potentials is evidenced by the larger oscillations in the tails of these GWF's compared to those of Fig. 2. Despite this, these GWF's have also essentially stabilized to the bulk Wannier function by the third site. These two sets of GWF's are plotted together to point up their similarity. The most apparent difference is that the surface GWF of the WA potential is displaced from zero (because the surface well of the WA potential is displaced from zero).

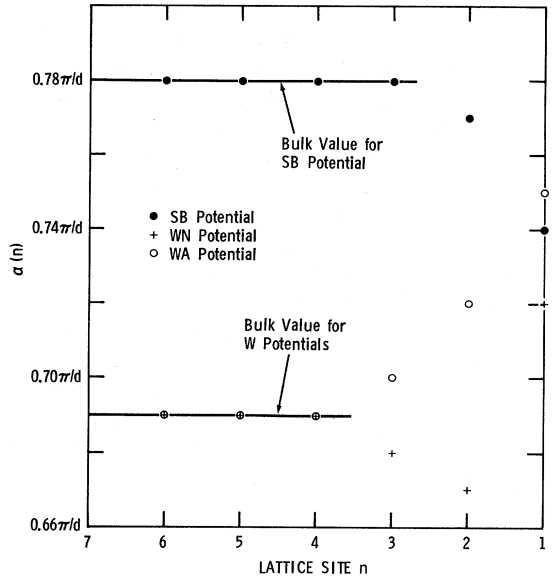

FIG. 4. Plot of the Gaussian parameters $\alpha(n)$ as a function of lattice site n for all three potentials. The parameters were determined to $0.01\pi/d$. The parameters revert to the bulk value within three sites for the SB potential and within four sites for the W potentials.

C. Accuracy

To assess the accuracy of the GWF's we wish to compare wave functions computed from them with exact wave functions calculated as described in Sec. II. A point-by-point comparison of individual wave functions is the most stringent possible test of accuracy. A calculation which proves accurate in this test will almost certainly give accurate values for observables such as energies, charge densities, and local densities of states. These are calculated by averaging over individual wave functions via expectation values and/or summing over wave functions. The exact solutions apply to an infinite crystal and ideally the approximate wave functions should also be calculated for an infinite crystal. Procedures exist for doing this,[3,7] but it is much easier to calculate approximate wave functions for a finite crystal. The wave functions (2.3) are then determined simply by solving a finite matrix eigenvalue equation,

$$\sum_{n'=1} \langle a_n(x)|H|a_{n'}(x)\rangle C_{n',q} = E_q C_{n,q}\,, \qquad (3.10)$$

of dimension equal to the number of sites N in the crystal. Since the wave functions are to be compared only over a few lattice sites in the surface region, the truncation of the sum in (3.10) beyond site N will not introduce serious errors provided N is large enough. We find that the truncation introduces no spurious surface states or long-range disturbances, and that a modest value of 20 for N is entirely adequate.

One effect of the truncation of the eigenvalue equation is that one obtains only N wave functions. In the case of the continuum states, there arises the question of which exact wave functions to compare them with. Two obvious choices can be made; one can compare wave functions of the same energy, or instead wave functions of identical k values. We have tried both ways and find little difference. We choose to present comparisons of wave functions of the same wave-vector magnitude.

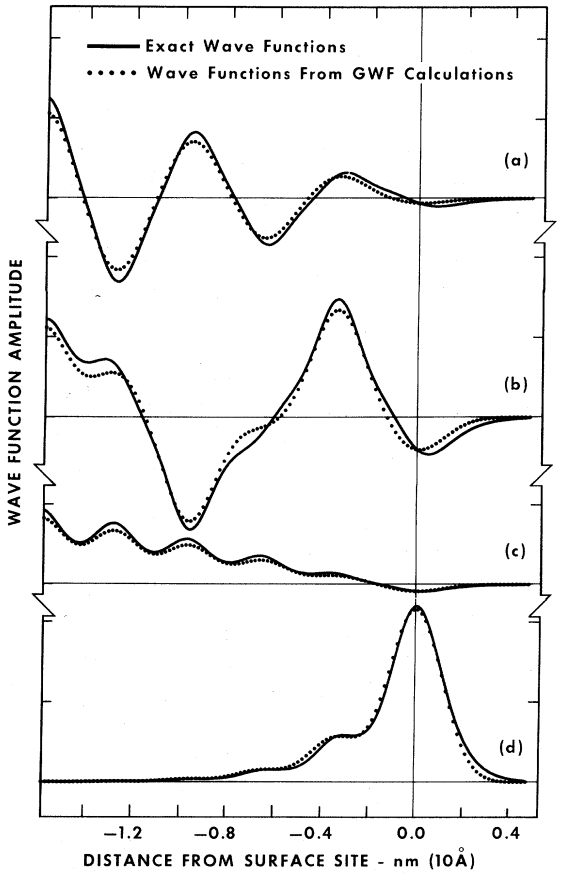

FIG. 5. Comparison of approximate with exact wave functions for the SB potential. The approximate wave functions were calculated from the GWF's of Fig. 2. The top three plots compare wave functions near the (a) top, (b) middle, and (c) bottom of the lowest band. The $|k|$ values associated with each pair of solutions, and the approximate and exact energies in eV are, respectively, (a) $0.9479\pi/d$, 5.640, 5.555; (b) $0.5539\pi/d$, 4.450, 4.323; and (c) $0.0509\pi/d$, 3.360, 3.344. The bottom plot compares the approximate and exact surface-state wave functions. The energies are respectively 2.770 and 2.734.

To make such a comparison with the exact solutions, we first calculate the approximate $E^0(k)$ from the familiar direct lattice expansion,

$$E^0(k) = \sum_n \langle a_0^0(x)|H^0|a_n^0(x)\rangle\, e^{ikn}. \qquad (3.11)$$

In (3.11), $a_n^0(x)$ is the approximate bulk Wannier function. Given an energy eigenvalue, one can determine the k value from (3.11). Then the corresponding exact solution can be picked out using that k value together with the exact $E^0(k)$ curve of the Mathieu potential.[16]

In Figs. 5–7 we compare the approximate wave functions calculated with simple Gaussians with exact wave functions for all three potentials.[19] The over-all agreement is quite good, and, based on a number of other comparisons, is typical of the accuracy to be expected for all wave functions. In light of the simplicity of the GWF calculations (which involve at most four parameters), the results of these most stringent tests of approximate quantum-mechanical calculations are remarkable. This quite satisfactory accuracy was obtained using only the lowest energy ("s-like") $g_n(x)$ as a trial function.

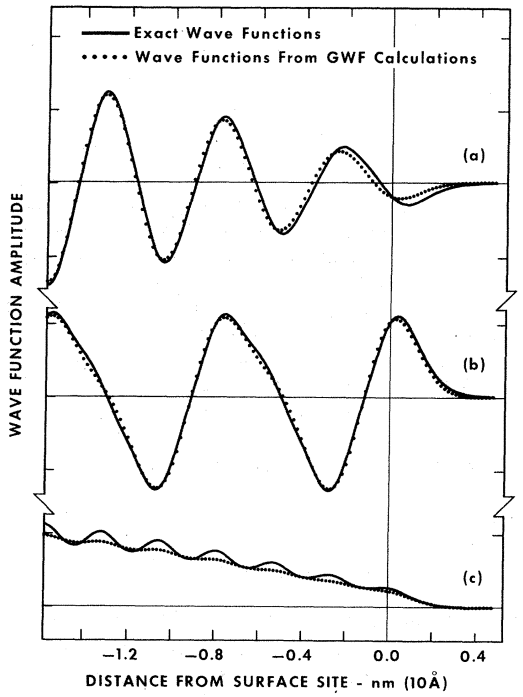

FIG. 6. Comparison of approximate with exact wave functions for the WN potential. The approximate wave functions were calculated from the "solid" GWF's of Fig. 3. The plots compare wave functions near the (a) top, (b) middle, and (c) bottom of the lowest band. The $|k|$ values associated with each pair of solutions, and the approximate and exact energies in eV are, respectively, (a) $0.9521\pi/d$, 6.650, 6.590; (b) $0.6621\pi/d$, 4.825, 4.750; and (c) $0.0467\pi/d$, 2.626, 2.530. This potential has no surface state.

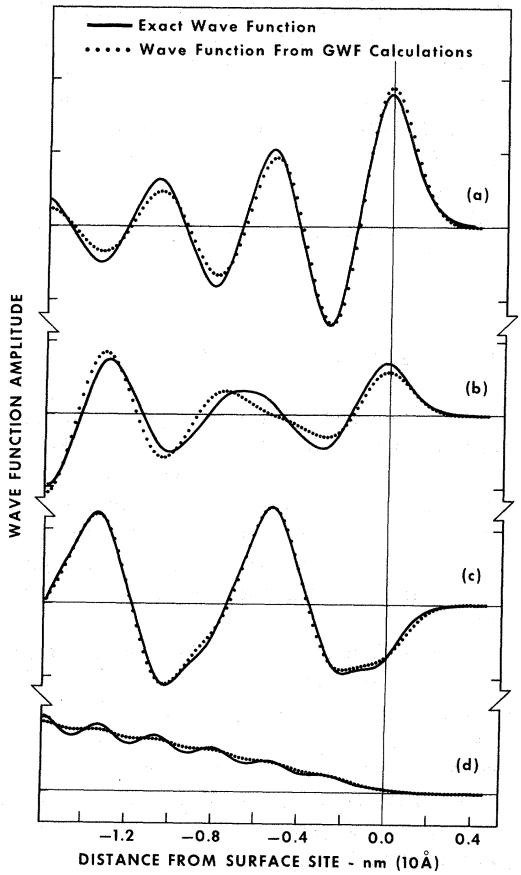

FIG. 7. Comparison of approximate with exact wave functions for the WA potential. The approximate wave functions were calculated from the "dotted" GWF's of Fig. 3 obtained with Gaussians. The top plot compares surface-state wave functions. The approximate and exact energies in eV are 7.051 and 6.955. The remaining plots compare wave functions near the (a) top, (b) middle, and (c) bottom of the lowest band. The $|k|$ values associated with each pair of solutions, and the approximate and exact energies are, respectively, (a) $0.9444\pi/d$, 6.628, 6.563; (b) $0.6404\pi/d$, 4.679, 4.611; and (c) (c) $0.0490\pi/d$, 2.627, 2.531.

Note that the surface state for the WA potential decays much more slowly to zero than does the charge density to its bulk value (see Sec. III B). There is a compensation here between the charge-density distribution of the surface state and that of the continuum states.

D. Extending the trial functions

Despite the very favorable results of the simple calculations described above, it is of interest to

see how well the GWF calculation converges to the the exact solutions when more flexible trial functions are used. Accordingly a calculation was done for the WA potential using linear combinations of harmonic oscillator wave functions[20] for the $g_n(x)$:

$$g_n(x) = \sum_j A_{n,j} u_j[\alpha_n(x-n)], \tag{3.12}$$

where

$$u_j(\alpha x) = (\alpha/\pi^{1/2}2^j j!)^{1/2} e^{-\alpha^2 x^2/2} H_j(\alpha x), \tag{3.13}$$

and where the $H_j(\alpha x)$ are Hermite polynomials. The parameters are the $A_{n,j}$ and the α_n. These trial functions represent an extension of the simpler calculations since $u_0(\alpha x)$ is a Gaussian. Remember that the harmonic-oscillator wave functions are analogs of atomic wave functions for the Mathieu potential [see discussion below Eq. (3.3)].

For the calculation of $g_n^0(x)$, the even functions u_0, u_2, u_4, u_6 were employed. Four parameters were involved: the three independent A's and a single scale factor α. For the surface calculation the first five $g_n(x)$ closest to the surface were allowed to differ from $g_n^0(x)$. For example, $g_1(x)$ was represented by the functions u_0 through u_6, the odd functions being included to allow for asymmetry. A total of 31 parameters were involved. A comparison of exact wave functions with wave functions obtained from this GWF calculation is shown in Fig. 8. Note that the wave functions are converging to the exact solutions with even greater accuracy than in Figs. 5–7.

An exact Wannier function for the Mathieu potential can be calculated by Fourier composition of its eigenfunctions.[15,16] This particular one of the many exact Wannier functions decays asymptotically as an exponential since it satisfies the conditions described by Kohn,[21] namely, it is real, symmetric, and is obtained from wave functions (of his type $A1$) which are continuous functions of k. This exact Wannier function for the W potential is shown in Fig. 9, where it is compared with the one-parameter and four-parameter approximate Wannier functions. Note that while both approximate functions agree quite well with the exact function over the large central peak, they are more localized having noticeably more rapidly decaying tails. In this connection, note also that all of the approximate $a_n(x)$ calculated here decay asymptotically as Gaussians (since they are linear combinations of terms containing Gaussian factors). Thus they do not exhibit the exponential behavior at infinity proved for the exact $a_n(x)$.[3-5]

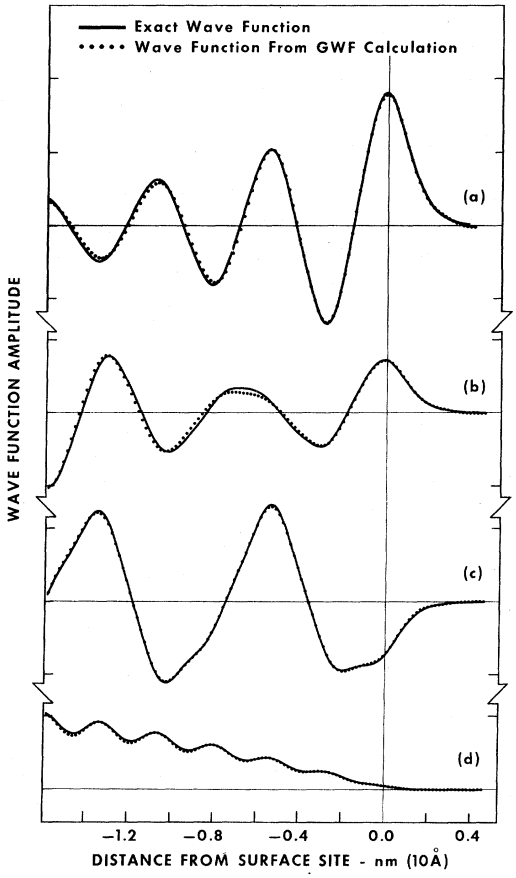

FIG. 8. Comparison of approximate with exact wave functions for the WA potential. The approximate wave functions were calculated from the GWF's obtained with the 31-parameter calculation. The top plot compares surface-state wave functions. The approximate and exact energies in eV are 6.973 and 6.955. The remaining plots compare wave functions near the (a) top, (b) middle, and (c) bottom of the lowest band. The $|k|$ values associated with each pair of solutions, and the approximate and exact energies are, respectively, (a) $0.9422\pi/d$, 6.572, 6.554; (b) $0.6388\pi/d$, 4.608, 4.603; and (c) $0.0497\pi/d$, 2.536, 2.532. Convergence toward the exact solutions is apparent.

IV. CONCLUDING REMARKS

The principal consequences of this work are as follows: (i) The GWF calculations give accurate results with simple atomlike trial functions. This is important because it implies that the basic form of the trial functions can be inferred from the atomic orbitals of the constituent atoms. (ii) The GWF's decay very rapidly to the bulk Wannier functions on moving into the crystal from the surface. Thus only a few $a_n(x)$ in the surface region need be different from the bulk $a_n^0(x)$. This implies that the charge density also damps rapidly to its bulk value.

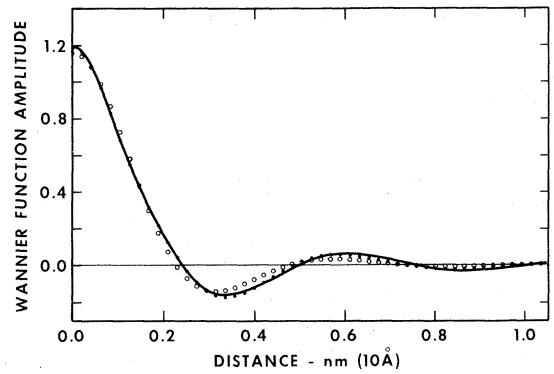

FIG. 9. Comparison of the one-parameter (open circles), and the four-parameter (solid circles) approximate bulk Wannier functions with an exact Mathieu-Wannier function (solid curve) for the W potential. This latter fuuction is the unique Wannier function which is real, symmetric, and decays asymptotically as an exponential (see text).

These facts, which would be anticipated for tightly bound electrons, hold even in the case of weak potentials in which the electrons are nearly free.

Three-dimensional systems of course present additional complexities as discussed in Ref. 7. Nevertheless, the one-dimensional results are encouraging and are evidence that the GWF formalism will provide a practical, efficient calculational technique for solid surfaces. We believe that the GWF approach is especially suited to the problem of calculating the electronic structure of transition-metal surfaces. The conduction bands of these materials are hybridized mixtures of relatively tightly bound *d* electrons and relatively free *s* electrons. One expects the GWF approach, since it is based on atomlike functions, to *ipso facto* deal efficiently with tightly bound electrons, and the test calculations imply that it can handle nearly free electrons efficiently as well.

Currently, we are applying the GWF formalism to systems involving simple- and transition-metal surfaces.

ACKNOWLEDGMENTS

We would like to thank W. Kohn, E. W. Plummer, G. G. Kleiman, F. A. Arlinghaus, and J. C. Tracy for helpful conversations. Programming assistance from J. C. Price is gratefully acknowledged.

[1]H. D. Hagstrum and G. E. Becker, Phys. Rev. B 8, 1580 (1973).
[2]D. E. Eastman and W. D. Grobman, Phys. Rev. Lett. 28, 1378 (1972).
[3]W. Kohn and J. Onffroy, Phys. Rev. B 8, 2485 (1973).
[4]J. J. Rehr and W. Kohn, Phys. Rev. B 9, 1981 (1974).
[5]J. J. Rehr and W. Kohn, Phys. Rev. B 10, 448 (1974).
[6]J. R. Smith and J. G. Gay, Phys. Rev. Lett. 32, 744 (1974).
[7]J. G. Gay and J. R. Smith, Phys. Rev. B 9, 4151 (1974).
[8]G. F. Koster, Phys. Rev. 95, 1436 (1954).
[9]W. Kohn, Phys. Rev. B 1, 4388 (1973).
[10]Philip W. Anderson, Phys. Rev. Lett. 21, 13 (1968); Phys. Rev. 181, 25 (1969); J. D. Weeks, P. W. Anderson, and A. G. H. Davidson, J. Chem. Phys. 58, 1388 (1973).
[11]P. O. Löwdin, J. Chem. Phys. 18, 365 (1950).
[12]R. Haydock, V. Heine, M. J. Kelly, and J. B. Pendry, Phys. Rev. Lett. 29, 868 (1972); R. Haydock, V. Heine, and M. J. Kelly, J. Phys. C 5, 2845 (1972).
[13]W. Kohn, Phys. Rev. B 10, 382 (1974).
[14]P. M. Morse and H. Feshbach, *Methods of Theoretical Physics* (McGraw-Hill, New York, 1953), Pt. II, p. 1650.
[15]J. C. Slater, *Symmetry and Energy Bands in Crystals* (Dover, New York, 1972), Chap. 6.
[16]J. C. Slater, Phys. Rev. 87, 807 (1952).
[17]V. Halpern, J. Phys. C 3, 1900 (1970).
[18]C. Kittel, *Quantum Theory of Solids* (Wiley, New York, 1963), p. 274.
[19]The exact continuum wave functions were δ-function normalized, i.e., the Mathieu functions of which they were composed were δ-function normalized. To achieve approximate δ-function normalization of the approximate wave functions, the "box"-normalized solutions to (3.10) were multiplied by $(Nd)^{1/2}/(2\pi)^{1/2}$.
[20]L. I. Schiff, *Quantum Mechanics* (McGraw-Hill, New York, 1955), p. 64.
[21]W. Kohn, Phys. Rev. 115, 809 (1959).